scientific reports

Check for updates

OPEN

Mixed matrix membrane of poly(4-methyl-1-pentyne) and ZIF-8 for enhanced CO_2 separation over H_2 and CH_4

Behnam Majid-Nateri, Reza Abedini✉ & Alireza Amiri

Carbon dioxide (CO_2) generally exists as the main impurity in natural gas, whose main component is methane. The presence of CO_2 reduces the energy content of natural gas and also causes the corrosion of pipelines. To prevent such problems, natural gas must contain a small concentration of CO_2 (less than 2% by weight). Membrane technology is an attractive separation method that has been widely studied due to its advantages such as high efficiency, low operating costs, and low energy requirements. However, in the last decade, Mixed Matrix Membranes (MMMs) have attracted the attention of many researchers due to their suitable capabilities in separating polar from non-polar gases. In this research, a new MMMs was obtained by adding imidazole zeolite nanoparticle (ZIF-8) to the poly methyl pentene (PMP) polymer matrix. The polymer part of this membrane can provide high permeability and suitable mechanical and thermal stability. In addition, ZIF-8 particles enhance CO_2 separation by offering high CO_2 adsorption capacity and molecular sieving, improving selectivity. The gas permeability test was performed on pure and mixed matrix membranes at 30 ℃ and pressures of 2, 6 and 10 bar. In addition, the fabricated membranes were evaluated by FESEM, FTIR-ATR, BET, DMA and TGA tests. The results indicated that in the MMMs containing 30 wt% of nanoparticles in the polymer, the permeability of CO_2 gas improved by more than 180% and reached about 278.95 barrer, compared to the pure polymer membrane at a pressure of 10 bar. Moreover, the selectivity of CO_2/CH_4 and CO_2/H_2 increased by 142% and 155%, respectively, primarily due to the preferential sorption of CO_2 over H_2 and CH_4 facilitated by ZIF-8 particles.

Keywords Reverse selectivity, Mixed matrix membrane, Poly Methyl pentene, CO_2 separation

Separation processes have always been significantly important in the oil, gas and petrochemical industries, and various methods have been used for this purpose. Gases are used in large quantities in various industries, and this further specifies the necessity of purification and separation of gases from the gas mixture[1]. One of the most important processes in the gas industry is gas sweetening, in which CO_2 and hydrogen sulfide (H_2S) are separated from natural gas (CH_4). The presence of CO_2 gas in the pipeline along with natural gas causes pipe corrosion, formation of gas hydrates and loss of gas transmission energy[2]. Therefore, the separation of CO_2 from natural gas in order to increase the calorific value of the gas and also to prevent the abovementioned issues, is a very important process in separation and transmission. Although the separation process is one of the most expensive steps of any chemical and petrochemical industry, a huge part of the cost of a product covers the separation process and the required equipment due to the high significance of this process. As a result, finding a cheaper and simpler separation method can be of great importance[3]. So far, various methods have been investigated for the removal and separation of CO_2, including: absorption, cryogenic processes (with and without distillation), surface adsorption (thermal and pressure swing adsorptions) and membrane-based processes, from which the latter is a new and emerging technology compared to the rest of the mentioned methods[4]. In Membrane-based processes, gases are purified (separated from each other) with the aid of a permeable membrane, and different driving forces such as pressure, concentration and electric potential differences[5]. The advantages of this process over other methods is low energy consumption, suitable mass transfer rate, rapid membrane separation, no need for complex equipment and versatile installation and operating conditions[6]. Among different membranes, polymer membranes have attracted the attention of many researchers due to their low operating cost, variable and

Enhanced Oil Recovery and Gas Processing Research Lab, Faculty of Chemical Engineering, Babol Noshirvani University of Technology, Babol, Iran. ✉email: abedini@nit.ac.ir

flexible design, cost-effective production along with easy construction[7]. However, regardless of all the advantages that polymer membranes could provide, they suffer from limitations and weaknesses in gas separation, the most important of which is the inverse relationship between the two parameters of selectivity and permeability. This means that high permeability and selectivity cannot be expected from polymers at the same time. Mixed matrix membranes (MMMs) are composed of a continuous polymer phase serving as the base and a dispersed phase, which may include zeolites, molecular sieves, or nano-sized particles. These membranes have been developed to enhance the gas separation performance of polymeric membranes[8].

Among the types of gas separator membranes and especially polymer membranes, MMMs are particularly important because they have the ability to approach and overcome the Robson limit in gas separation[9]. Studies conducted on MMMs showed that their performance is not just adding the inherent characteristics of a particular phase. Various factors such as the correct selection of polymer and additives, the interface between particles and polymers, sedimentation and distribution of particles and particle size can affect the performance[10]. The type of the additive (dispersed phase) is known to be the most important factor in the development of MMMs. Therefore, researchers applied different nanoparticles, among which the best results were obtained with metal-organic frameworks. Metal-organic frameworks (MOFs) are a new emerging class of porous crystalline materials with one, two, or three-dimensional network, composed of metal ions or clusters with monodentate or polydentate organic linkers. These frameworks are highly compatible with polymer chains because they have various organic groups which can reduce the non-selective holes in the polymer-particle interface[11]. These MOFs have impressive merits including low density, flexibility and high specific surface (in energy storage technology, filtration and building production from lightweight materials), completely regular and uniform cavities, high porosity and chemical stability. The abovementioned properties are important factors for increasing the gas selectivity of MMMs and the reason for the superiority of this category of materials over zeolites and carbon materials[12].

Zeolite imidazole frameworks-8 (ZIF-8) are a subset of MOFs, formed in a tetrahedral arrangement, where the metal clusters are connected by imidazole linkers. These particles can provide high surface area (due to the presence of transition metals such as cobalt), the ability to adjust the cavity, high crystallization, mechanical, thermal and chemical stability, versatility and functionalization for various application fields. Moreover, the high penetration and adsorption capability of these frameworks toward specified molecules enhances their flexibility during the adsorption process and therefore can be considered a good addition in the formation of MMMs[13].

Another noteworthy point in the performance of MMMs is the type of the polymer. One of the most promising, commercially available polymers for membrane fabrication is poly methyl pentene polymer (PMP). PMP, also known as TPX, is an amorphous polymer based on acetylene (poly acetylene polymers have the highest permeability rate among known materials). In addition, this polymer is part of the polyolefin family, with glass transition temperature of 20 to 30 ℃ and crystallinity degree of 20 to 80%. PMP has a low density of 0.78 g per cubic centimeter, a fractional free volume of above 0.28 and the softening temperature of about 250 ℃. It is also the most permeable pure hydrocarbon-based polymer known, due to its very high free volume. Other notable properties include high chemical resistance, high thermal stability, and good permeability[14].

The membranes generally used in the gas separation process are divided into two groups. The first group are conventional selective membranes in which the separation is based on the size and penetration rate of the particle inside the membrane. The second group are non-conventional reverse selective membranes with separation criterion based on the solubility of the particle inside the membrane.

In general, the solution-diffusion model is widely used for the gas transport mechanism in dense polymer membranes. According to this model, as shown in "equation (1)" gas permeability (P) is equal to the product of permeability (D) and solubility (S).

The permeability unit is 1 Barrer = 1×10^{-10} cm^3 (STP) cm/cm^2 s cmHg.

$$P = S \times D \tag{1}$$

The ability of the membrane to separate different gases, for instance, components A and B, is equal to the permeability ratio of those two components, which is called selectivity (membrane separation factor). It is obtained according to the "equation (2)":

$$\alpha_{A/B} = \frac{P_A}{P_B} \tag{2}$$

According to "equation (3)" the ideal selectivity of two gases (A/B) is the product of solubility selectivity (S_A/S_B) and diffusivity selectivity (D_A/D_B). To obtain the optimal separation factor, the above two fractions must be complementary. Therefore, the permeability of the gas components could not only be attributed to the difference in the diffusion coefficient of the penetrant (diffusivity selectivity). The difference in chemical and physical interactions of these components with the polymer (solubility selectivity) should also be taken into consideration in the overall gas selectivity. The separation factor of a component in a gas mixture are determined by the balance between these two parameters[15,16].

$$\alpha_{A/B} = \frac{P_A}{P_B} = \left(\frac{S_A}{S_B}\right) \times \left(\frac{D_A}{D_B}\right) \tag{3}$$

Polymers with flexible chains possess high free volume (the space which is not occupied by polymer chains) while they have weak screening property based on size. In this regard, the passage of molecules through the membrane is facilitated and accelerated in larger polymers with increased free volume. Glassy polymers such as

PTMSP, PMP, AF2400, PIM-1, etc. provide high permeability for larger condensable gases, due to the significant free volume[17]. In reverse selective membranes, the gases are separated based on their solubility in the membrane. Also, the features of the membranes have direct relationship with the free volume, therefore, it is possible to increase the free volume of the desired polymer by breaking polymer chains[18]. According to the free volume criteria, the reverse selectivity phenomenon can be justified with the help of this statistical mechanics model[19], according to which, the diffusion coefficient of a component in the porous space is obtained from "equation (4)":

$$D_i = \sigma \exp\left(\frac{-\gamma \nu_i}{V_{FV}}\right) \tag{4}$$

where, σ and γ (overlapping factor) are positive constants, v_i is the minimum desired space (minimum empty volume) for component A to penetrate the polymer, D_i is the penetration coefficient of the desired component, and V_{FV} is the average free volume (average void volume) of the polymer. Adding "equation (4)" to "equation (3)" indicates that the selectivity of D_A/D_B is proportional to $\exp\left(\frac{-\gamma \nu_i}{V_{FV}}\right)$. On the other hand, the value of v_i is much smaller than V_{FV}, so as the V_{FV} increases, the $\left(\frac{-\gamma \nu_i}{V_{FV}}\right)$ tends to zero and $\left(\frac{-\gamma \nu_i}{V_{FV}}\right)$ approaches one. As a result, the D_A/D_B ratio tends to one with the increase of the free volume of the polymer. Therefore, the improvement of selectivity due to the increase in the free volume of polymers could be validated based on the statistical mechanics model of Cohen and Turnball[16].

Accordingly, the aim of this work is to develop a new reverse selective membrane comprising high free volume polymer and MOF particles. PMP is used as a polymer phase of MMM and the synthesized ZIF-8 particles used as a dispersed phase within the membrane matrix. The combination of PMP and ZIF-8 enables reverse selectivity for CO_2 separation due to the high free volume of PMP, which facilitates solubility-driven transport rather than size-sieving, allowing CO_2 to permeate faster than smaller gases like H_2 or larger CH_4. ZIF-8, with its flexible pore apertures, exhibits a gate-opening effect that preferentially allows CO_2 diffusion while restricting larger or less condensable gases. This synergy between PMP's intrinsic high permeability and ZIF-8's selective adsorption and diffusion mechanisms results in enhanced CO_2 permeability, leading to reverse selectivity. A comprehensive characterization studies (i.e., FESEM, FTIR-ATR, BET, DMA and TGA) employed to study the physical properties of membranes. Moreover, a series of gas permeation tests including CO_2/CH_4 and CO_2/H_2 separation were designed over the different feed pressure to examine the gas separation performance of resulting MMMs.

Experimental

Materials

Poly methyl pentene polymer (PMP), in the form of milky pellets with low molecular weight was purchased from Sigma-Aldrich to be used as the polymer phase of the membrane. Carbon tetrachloride (CCl_4) with a purity of 99.5% was purchased from Merck and used as a solvent of PMP. Likewise, ZIF-8 porous nanoparticles were synthesized and used as additives, using 2-methylimidazole, zinc nitrate and methanol purchased from Merck.

Synthesis of ZIF-8

In order to synthesize ZIF-8 nanoparticles, first, 2-methylimidazole (6.48 g) and zinc nitrate (2.933 g) were separately dissolved in 200 ml of methanol. The 2-methylimidazole solution was slowly poured into the zinc nitrate solution and stirred for 1 h. The final solution rested for 24 h and then centrifuged for 10 min at 10,000 rpm. Finally, after a sedimentation process of 12 h, the samples were washed three times by fresh methanol to remove unreacted precursors, organic molecules, or other residues. Finally the obtained clean solids were dried in an oven at a temperature of 65 ℃ for 12 h[20].

Membrane preparation

Initially, the PMP polymer was placed in the oven at 60 ℃ for 6 h to remove any possible moisture. Then 5.7 gr of CCl_4 solvent was added into a container with a gasketed lid and placed in an oil bath. The entire set was placed on a magnetic stirrer followed by the addition of 0.3 gr of the polymer in three separate steps (to prevent polymer aggregation). Next, the polymer solution samples were casted on a smooth, clean, glass plate using a film applicator with the thickness of 40 μm. The casted films were placed in an oven at a temperature of 50 ℃ for 6 h in order to completely evaporate the solvent. In case of the mixed matrix membrane, the manufacturing process was almost the same as the pure membrane. Only the dispersion of the additive nanoparticles in the CCl_4 solvent was added to the overall process. In this regard, in the added step, ZIF-8 particles with different weight percentages were exposed to ultrasonic waves in the solvent for 10 min in order to avoid the non-uniform distribution of the particles. Next, the polymer was added step by step to the solution under stirring, same as the pure membrane method. Table 1 shows the percentage composition of each of the cast membranes[21].

Membrane characterization

To determine the characteristic bonds in the prepared membranes, Fourier transform infrared spectrometry (FTIR-ATR) in the wave number range of 400–4500 cm^{-1} and resolution of 4 cm^{-1} was recorded on JASCO Model 300, Japan, system. Moreover, in order to monitor the surface and transverse structure of the obtained membranes, as well as the dispersion of nanoparticles in the polymer substrate, Field Emission Scanning Electron Microscopy (FESEM) was performed by MIRA3 TESCAN (Czech) device. In the sample preparation step, the pure and the mixed matrix membranes were broken in liquid nitrogen and then covered with gold under argon gas in order to achieve a suitable cross-sectional area and therefore proper resolution. The N_2 adsorption-desorption test is based on measuring the volume of nitrogen gas absorbed and desorbed by the

Membrane code	Polymer (3 wt%)		Solvent (wt%) CCl_4
	PMP	ZIF-8	
M1	100	0	97
M2	90	10	97
M3	80	20	97
M4	70	30	97

Table 1. Solution composition of pure and MMMs membranes.

surface of the material, at a constant temperature of liquid nitrogen (77 K). Based on the measured absorption and desorption values of the material, this system can calculate the specific surface, the total volume of the holes and the average size of the holes of the material with the aid of Brunauer-Emmett-Teller (BET) theory. The device used in this test was the Belsorp mini II manufactured by the Japanese company Japan Bel. To investigate the degradation temperature and the effect of additives on the thermal behavior of mixed matrix membrane samples, TGA thermogravimetric analysis was conducted using TGA-50 device, Shimadzu. The nitrogen gas was applied at the heating rate of 10 ℃ per minute and the temperature range of 0 to 800 ℃. To investigate the glass transition temperature (T_g) and the mechanical properties of the membranes, mechanical dynamic analysis (DMA) was performed using the Pyris Diamond, USA device at a temperature range of 0 to 90 ℃ and a heating rate of 5 ℃/min. In order to measure the Young's modulus of the samples, the temperature was increased from 25 to 200 ℃ with a repetition rate of 5 ℃/min. Tensile strength and elongation at break were calculated at a temperature of 25 ℃ and with an increased force of up to 20 N.

Gas permeability measurements

The system commonly used to identify the permeability of the constructed membranes is a constant volume/variable pressure system, which has the ability to measure permeability at different temperatures and pressures. According to this system, the desired membrane is placed between two steel discs (permeable cells) which are connected to each other, and the high-pressure gas hits the membrane from the feed side. The gas passing through the membrane enters a chamber of fixed volume, which increases the pressure inside the chamber with time. This pressure increase is accurately recorded by pressure sensors, and the amount of pressure variation is obtained in terms of time. Permeability of passing gas at 2, 6 and 10 bar pressure is calculated through "equation (5)":

$$P(barrer) = \frac{273.15 \times 10^{10} VL}{760AT\left[\left(P_o \times 76\right)/14.7\right]}\left(\frac{dp}{dt}\right) \tag{5}$$

where, P is the gas permeability (Barrer), V is chamber volume (cm^3), L is the membrane thickness (cm), A is the surface area of the membrane (cm^2), T is the test temperature (k), P_o is gas feed pressure to the system (psia) and $\left(\frac{dp}{dt}\right)$ is the slope of the permeability gas pressure variation versus time.

To determine the selectivity of CO_2 over CH_4 and H_2 in mixed matrix membranes (MMMs), the permeabilities of CO_2, CH_4, and H_2 are measured individually under identical conditions. Selectivity is then calculated by dividing the permeability of CO_2 by that of CH_4 to obtain CO_2/CH_4 selectivity, and by dividing the permeability of CO_2 by that of H_2 to obtain CO_2/H_2 reverse selectivity. The gas diffusion coefficient (D) (cm^2/s) was calculated using the vacuum time lag method (Eq. 6):

$$D = \frac{L^2}{6\theta} \tag{6}$$

where θ is the gas time lag (s), determined by extrapolating the linear region of the pressure-time diagram.

By referencing Eq. 1 and incorporating the gas diffusion properties obtained from Eq. 6, the gas solubility (cm^3(STP)/cm^3·cmHg) can be calculated accordingly:

$$S = \frac{P}{D} \tag{7}$$

Results and discussion

Fourier transform infrared spectroscopy – attenuated total reflectance (FTIR-ATR)

FTIR-ATR spectrum of additive particles, pure polymer membranes and mixed matrix membranes with different percentages of 10, 20 and 30% were recorded in the range of 400–4500 cm^{-1} and the results depicted in Fig. 1. According to the Fig. 1, in the spectrum of ZIF-8 particles, the peak at 421 cm^{-1} corresponds to the vibrational mode of Zn-N bond. The bands that appeared in the areas below 800 cm^{-1} are often caused by the bending of the rings. A transition from 1143 to 1175 cm^{-1} was observed, which can be related to the change of imidazole state to imidazolate. Moreover, the absence of any peak at 1850 cm^{-1} confirms the formation of imidazolate[22]. The peak appearing at 1307 and 1421 cm^{-1} represents C-N and C = N bond, respectively[23]. On the other hand, the absorbed signals at 1580 cm^{-1} refer to the vibration of the rings. The stretching vibration of symmetric and asymmetric bonds of $-CH_2-$ also appeared in wave numbers of 2927 and 2957 cm^{-1}, respectively. Adsorption

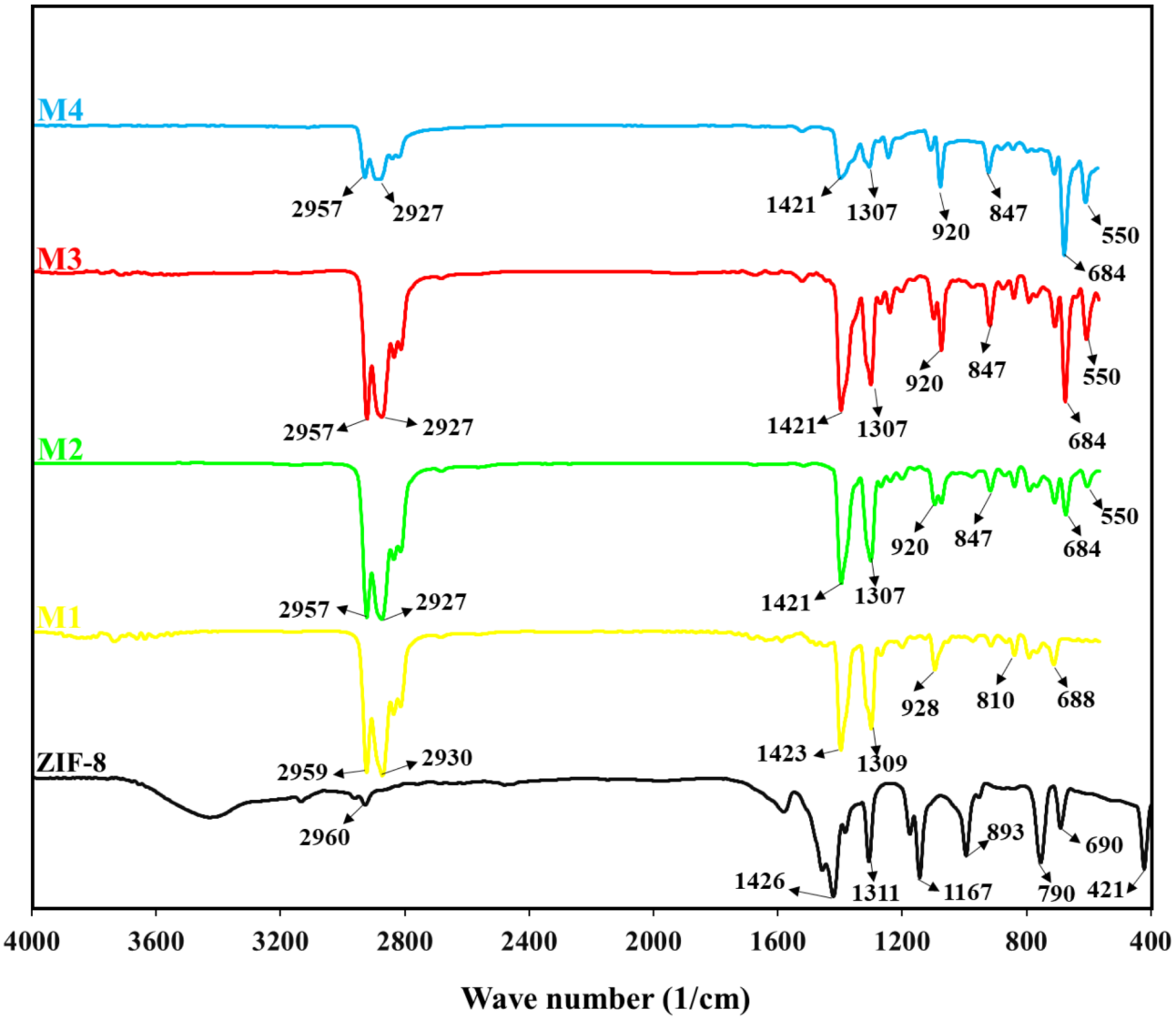

Fig. 1. FTIR spectra of ZIF-8, PMP (M1), PMP/10 wt% ZIF-8 (M2), PMP/20 wt% ZIF-8 (M3), PMP/30 wt% ZIF-8 (M4).

bands in the range of 2200 to 3300 cm^{-1} are related to the vibration of formed hydrogen bonds[24]. In the PMP spectrum, methyl groups attached to the polymer chain with asymmetric stretching vibrations are observed at 2903 and 2952 cm^{-1}. In addition, the peaks at 500 to 900 cm^{-1} are attributed to the symmetrical C-H bond. The stretching vibration of C-O-C is represented at 920 and 1167 cm^{-1}. MMMs also have the same bonds as pure polymer membranes. Due to the possible interactions between ZIF-8 and the polymer chains, the peaks characterizing these bonds are slightly shifted. An example of this displacement can be seen in the range of C-H and C-O-C bonds, which is also observed with some displacement in the MMMs, according to the figure[25].

Field emission scanning electron microscopy (FESEM)

In order to check the morphology of the synthesized membranes, the dispersion quality of nanoparticles and also to determine whether the constituents of the membranes are compatible with each other or not, the cross section of the membranes with different magnifications was tested by FESEM. The results are shown in Fig. 2. According to Fig. 2 (a), the pure polymer membrane has a uniform and dense structure with no defects. Figures 2 (b, c and d) illustrate the addition of ZIF-8 nanoparticles to the polymer matrix in which bright spots can be seen, representing the nanoparticles distributed in the dark space of the polymer. On the other hand, at higher weight percentages of additive particles, accumulation of particles was also observed. In addition, it is evident that the polymer/particle interface is of good quality and is almost free of any non-selective holes which can be attributed to the interaction between MOF organic groups and polymer chains. The cross-sectional images of the membranes with different weight percentages and in two different magnifications were also recorded. According to these images, as the weight% of ZIF-8 in the PMP network was raised, undesirable clusters of particles were

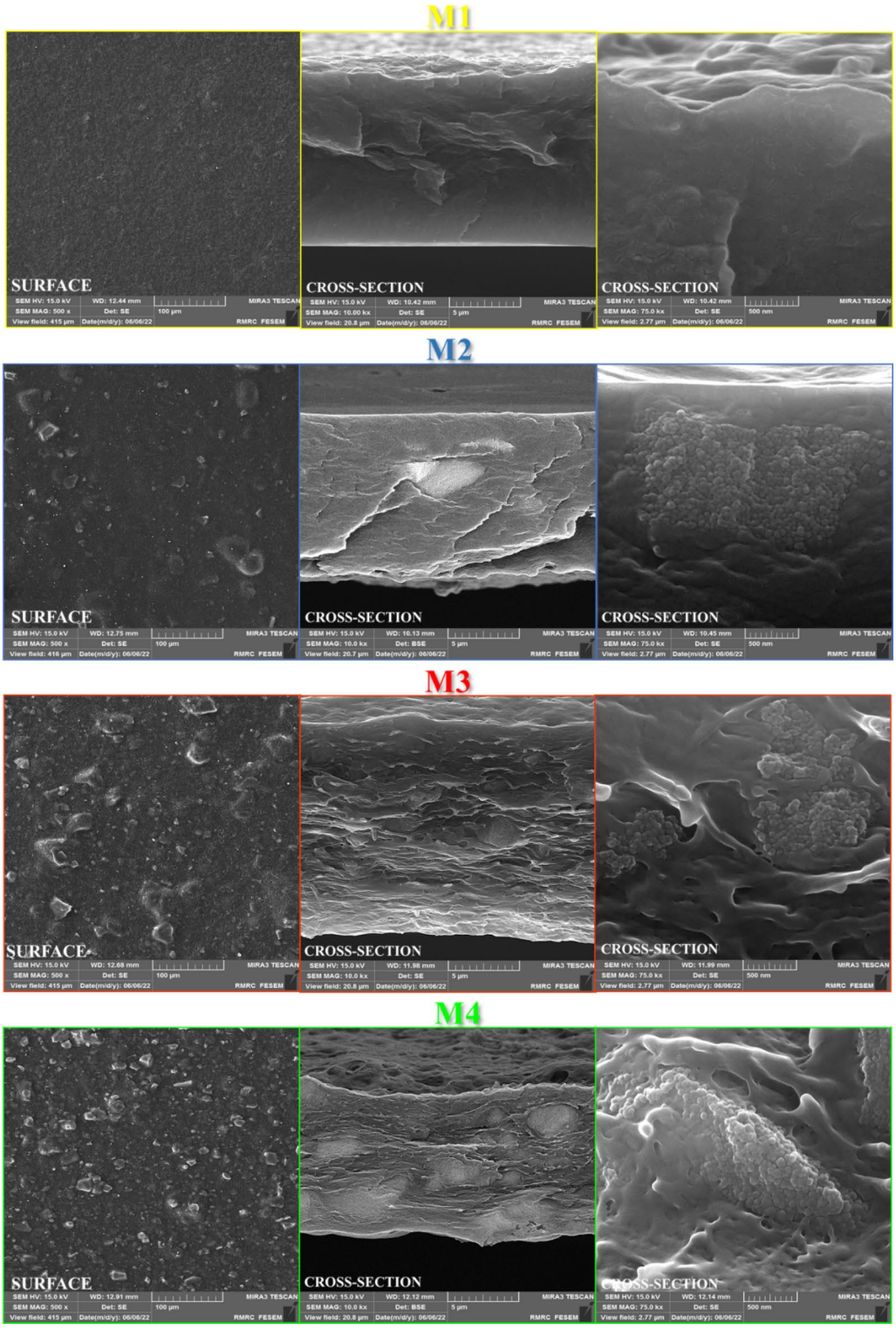

Fig. 2. The cross-sectional and surface images of (**a**) neat PMP, (**b**) PMP/ZIF-8 (10 wt%), (**c**) PMP/ZIF-8 (20 wt%), (**d**) PMP/ZIF-8 (30 wt%).

observed in the images. The accumulation of particles results in the formation of non-selective cavities, which correspondingly reduces the performance of the synthesized membranes[22,26,27].

N_2 adsorption-desorption analysis

In order to determine the structural characteristics of the synthesized ZIF-8 nanoparticles, the cell containing the desired sample was first placed in the liquid nitrogen tank. Then the amount of gas absorbed and desorbed by the

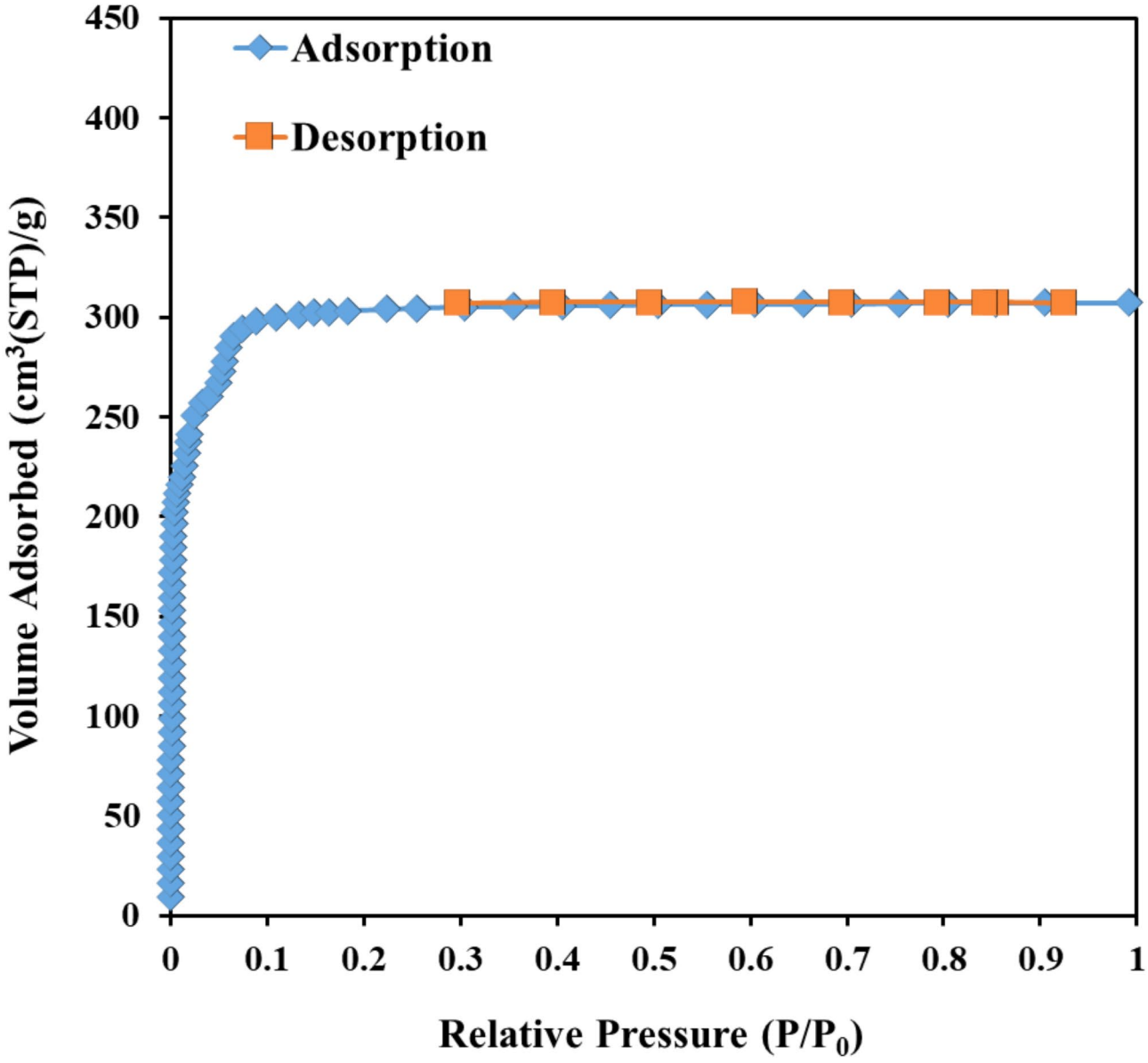

Fig. 3. N_2 adsorption–desorption of ZIF-8 at 77 k.

Sample	S_{BET} (m^2g^{-1})	V_{total} (cm^3g^{-1})	D_p (nm)
ZIF-8	1194.4	0.4751	1.5911

Table 2. BET analysis of ZIF-8 sample.

material was calculated by gradually increasing and decreasing the nitrogen gas pressure at each stage. Finally, the Nitrogen adsorption and desorption diagram was drawn at constant temperature of 77 K. According to the obtained diagram (Fig. 3), the behavior of all particles follows isothermal type 1, representing the microporous structure[28]. In the desorption diagram, no residual is observed, especially in the relative pressure of more than 0.4, which indicates very low number of interporosity (mesopore) in the particle structure. The most important feature of this isotherm is that, at low pressures, a rapid increase in adsorption is seen, and at high pressures, the curve becomes an almost horizontal line. This isotherm is also called Langmuir curve. In this curve, a monolayer adsorption occurs at low pressure, which indicates a strong interaction between the gas and the adsorbent surface. The properties of ZIF-8 nanostructure synthesized with methanol solvent, such as pore diameter, pore volume, and BET surface area are compiled in Table 2. The properties of ZIF-8 nanostructure synthesized with methanol solvent, such as pore diameter, pore volume, and BET surface area are compiled in Table 2. The results obtained from BET analysis indicate that the synthesized ZIF-8 exhibits a high specific surface area, which is a

characteristic feature of this material. Furthermore, the measured BET surface area values align well with those reported in previous studies, confirming the reliability and consistency of the synthesis method used in this work. This agreement suggests that the structural integrity and porosity of the synthesized ZIF-8 are comparable to those of ZIF-8 materials reported in the literature[29,30].

Thermogravimetric analysis (TGA)

The thermal behavior of the membranes prepared with different weight percentages of additive particles was studied with the aid of thermogravimetric decomposition test. TGA curves of ZIF-8 particles, PMP pure polymer and mixed matrix membranes are depicted in Fig. 4. The TGA diagram includes three parts: evaporation of moisture and solvent (in the temperature range of zero to 290 ℃), decomposition of polymer chains (in the range of 310 ℃) and decomposition of the organic part of the organic-metallic frameworks. Thermal degradation of PMP membrane chains started at a temperature of about 290 ℃. The degradation temperature (T_d) in the PMP/ZIF-8 composite network membrane increased as the weight% of ZIF-8 particles was raised, finally reaching an approximate temperature of 355 ℃. The increased destruction temperature of the membrane can be due to the interaction between the particles and the polymer matrix, which strengthens and hardens the polymer chains[31]. On the other hand, the strong covalent bond between nanoparticles and polymer reinforces the polymer chains and therefore more energy is required to break these polymer chains. The precise quantification of ZIF-8 loading

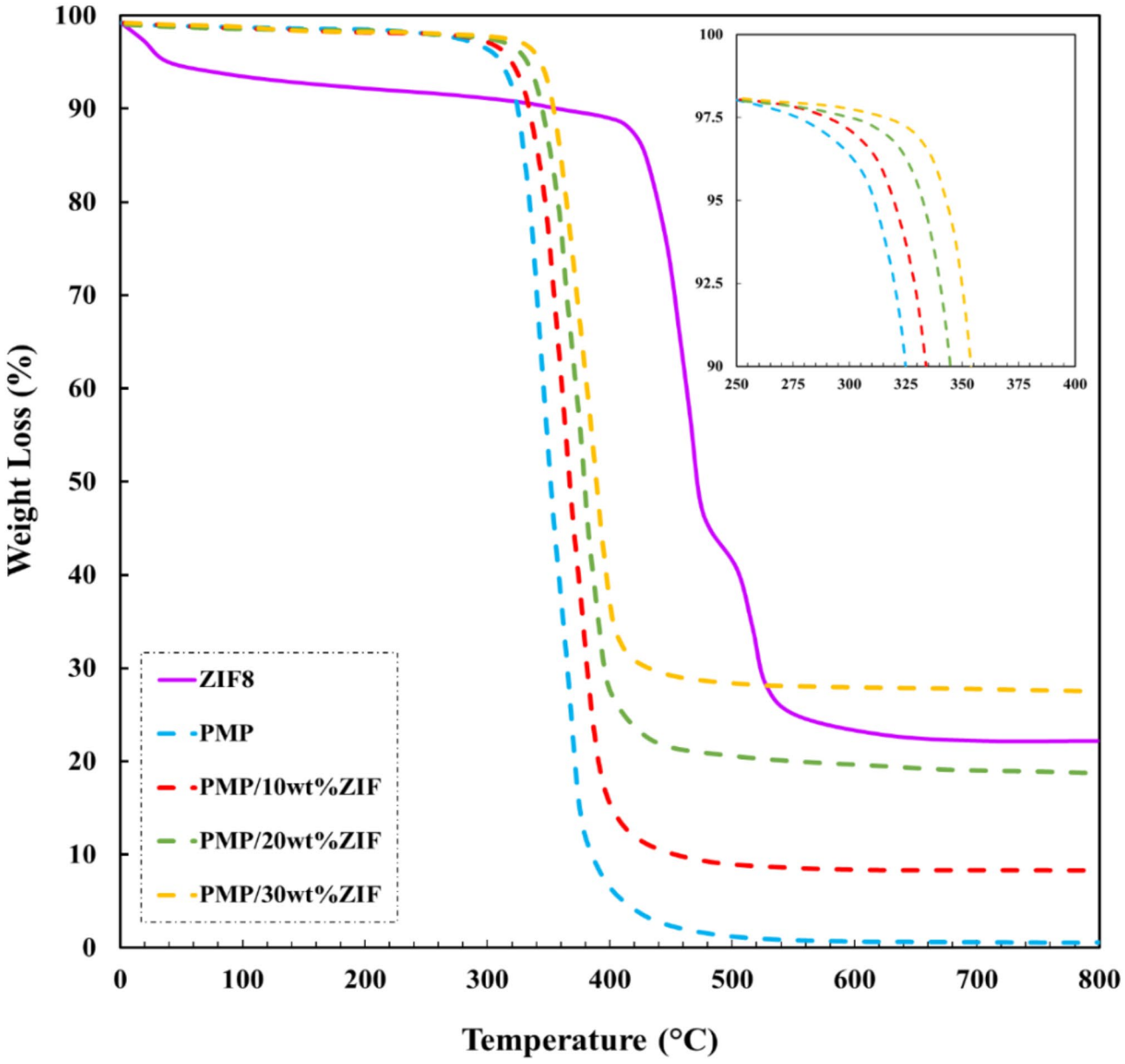

Fig. 4. Thermal gravimetric analysis (TGA) curve of ZIF-8 and MMMs with loading of 10, 20 and 30 wt% of MOF.

in MMMs was TGA analysis[33]. During the thermal decomposition process, the polymer matrix was completely degraded, leaving behind the inorganic ZIF-8 filler as a residual weight. The final residual weight% recorded in the TGA curves corresponds directly to the amount of ZIF-8 present in each membrane. By analyzing the residual mass at 800 °C, the calculated ZIF-8 loadings within the MMMs were determined to be 9.5 wt%, 19.7 wt%, and 28.9 wt%, corresponding to the M2, M3, and M4 membranes, respectively. These results confirm the effective incorporation of ZIF-8 into the polymer matrix and validate the reliability of the TGA method in accurately assessing the filler content in MMMs.

Dynamic mechanical analysis (DMA)

In this analysis, an oscillating force is applied to the sample and the response is evaluated. Figure 5 indicates the changes of tanδ and modulus (É) in terms of temperature for pure and mixed matrix membranes. The maximum of the tanδ diagram ($d \tan \delta / dT = 0$) represents the glass transition temperature (T_g) of the membranes. The peak located at 35 ℃ indicates the T_g of the PMP membrane, which is in accordance with previous reports[32]. Raising the weight% of ZIF-8 nanoparticles in the membrane increased the T_g values and the elastic modulus of the MMMs. This increase in T_g can be assigned to the confinement of polymer chains with ZIF-8 particles. The same is true for the elastic modulus, the presence of ZIF-8 nanoparticles strengthened the polymer chains. It should also be mentioned that at higher temperatures, the values of the elastic modulus of the MMMs reduced[33].

The mechanical properties of PMP membranes and composite networks containing 10, 20 and 30 wt% of ZIF-8 nanoparticles are summarized in Table 3. A reduction in the tensile strength and elongation at break was observed as the weight% of nanoparticles in the membrane was increased. The reduction in tensile strength with increasing ZIF-8 particle content in MMMs can be explained by several factors. Higher ZIF-8 content can increase brittleness by restricting the mobility of PMP chains, making the membrane more prone to fracture under stress. Furthermore, non-uniform dispersion of ZIF-8 particles at high loadings can cause agglomeration, leading to stress concentration points that reduce tensile strength. Contrary to tensile strength and elongation, Young's modulus increased in mixed matrix membranes. The increase in Young's modulus in mixed matrix membranes (MMMs), despite a reduction in tensile strength and elongation, can be explained by the incorporation of rigid filler particles (such as ZIF-8) into the polymer matrix. These particles act as a reinforcing phase, restricting the mobility of the polymer chains and making the membrane stiffer. As a result, the membrane resists deformation more strongly under stress, which leads to an increase in Young's modulus, a measure of stiffness.

Gas permeation results

The effect of nanoparticles on permeability and selectivity

The permeability values of CO_2, CH_4 and H_2 gases and the selectivity of CO_2/CH_4 and CO_2/H_2 in pure polymer membranes and mixed matrix membranes, at 30 ℃ and 2 bar pressure, are given in Table 4.

According to the data, for all the MMMs containing ZIF-8, the permeability values of CO_2 were significantly higher than the corresponding values of CH_4 and H_2, the values increased as the weight% of the additive was increased. For instance, in the PMP membrane, the permeability of CO_2, CH_4 and H_2 gases were 99.13, 7.38 and 8.52 Barrer, respectively, while the permeability values in the mixed matrix membrane containing 30 wt% of ZIF-8 particles enhanced to 259.81, 8.54 and 9.24 Barrer, respectively. Higher condensability and lower kinetic radius of CO_2 gas (the kinetic radius of CO_2 is equal to 0.33 nm and CH_4 is equal to 0.38 nm), compared to CH_4, along with the mutual effects between PMP polymer chains and CO_2 justifies the increased permeability toward CO_2. Likewise, this assertion is also true for H_2 gas (despite the kinetic radius of 0.29 nm, which is lower than CO_2). As illustrated in Fig. 6, increasing the weight% of ZIF-8 particles in the polymer network of the membrane improved the permeability of CO_2, CH_4 and H_2 gases. The obtained permeability of CO_2 gas is much higher in comparison to CH_4 and H_2 gases. Two factors are responsible for the improvement of CO_2 permeability in PMP/ZIF-8 mixed matrix membrane. First, the presence of ZIF-8 nanoparticles in the mixed matrix membrane increases the free volume of the membrane which facilitates higher condensability of CO_2. Second, the interaction between CO_2 gas quadrupoles with imidazolate linker in ZIF-8 nanoparticles leads to improved CO_2 permeability. On the other hand, unlike CO_2, the presence of ZIF-8 particles in the polymer matrix had much smaller effect on improving the permeability of CH_4 and H_2. This minor increase can be related to the weak absorption of these gases by ZIF-8 and the increased penetration in the polymer membrane due to the increased free volume of the polymer[34,35].

The effect of nanoparticles on permeability and solubility coefficients

Figure 7 depicts the values of diffusion coefficient and solubility of CO_2, CH_4 and H_2 in PMP polymer and mixed matrix membranes. Gas penetration and solubility in the membrane are the two influential factors in gas permeability. The diffusion coefficient values of all three gases increase in exchange for increasing the weight% of ZIF-8 nanoparticles, which can be due to the escalated free volume of the polymer. It should be taken into consideration that the presence of ZIF-8 nanoparticles elongates the gas penetration path and therefore can diminish the permeability. In general, the explanation of how the gases penetrate in the MMMs is somehow complicated and it is not possible to provide a conclusive verification of their behavior. In addition, the penetration of a gas in the membrane is a function of its molecular size, therefore, CO_2 gas passes through the space in the membrane more easily due to its smaller molecular size, in comparison to the other two gases. Gas solubility values in MMMs were higher than the corresponding values in PMP polymer membrane. The solubility coefficient of CO_2 in the PMP/ZIF-8 membrane increased from 15.96 to 30.32 (about 90%), while a very small improvement was observed in the solubility coefficient of CH_4 and H_2. The significant increase in CO_2 solubility in the presence of ZIF-8 particles can be attributed to the high tendency of this nanoparticle to absorb CO_2 and the greater condensability of CO_2 in the polymer matrix. The reason for this high affinity is the interaction between stable CO_2 quadrupoles with the imidazolate linker in ZIF-8. The lack of interaction

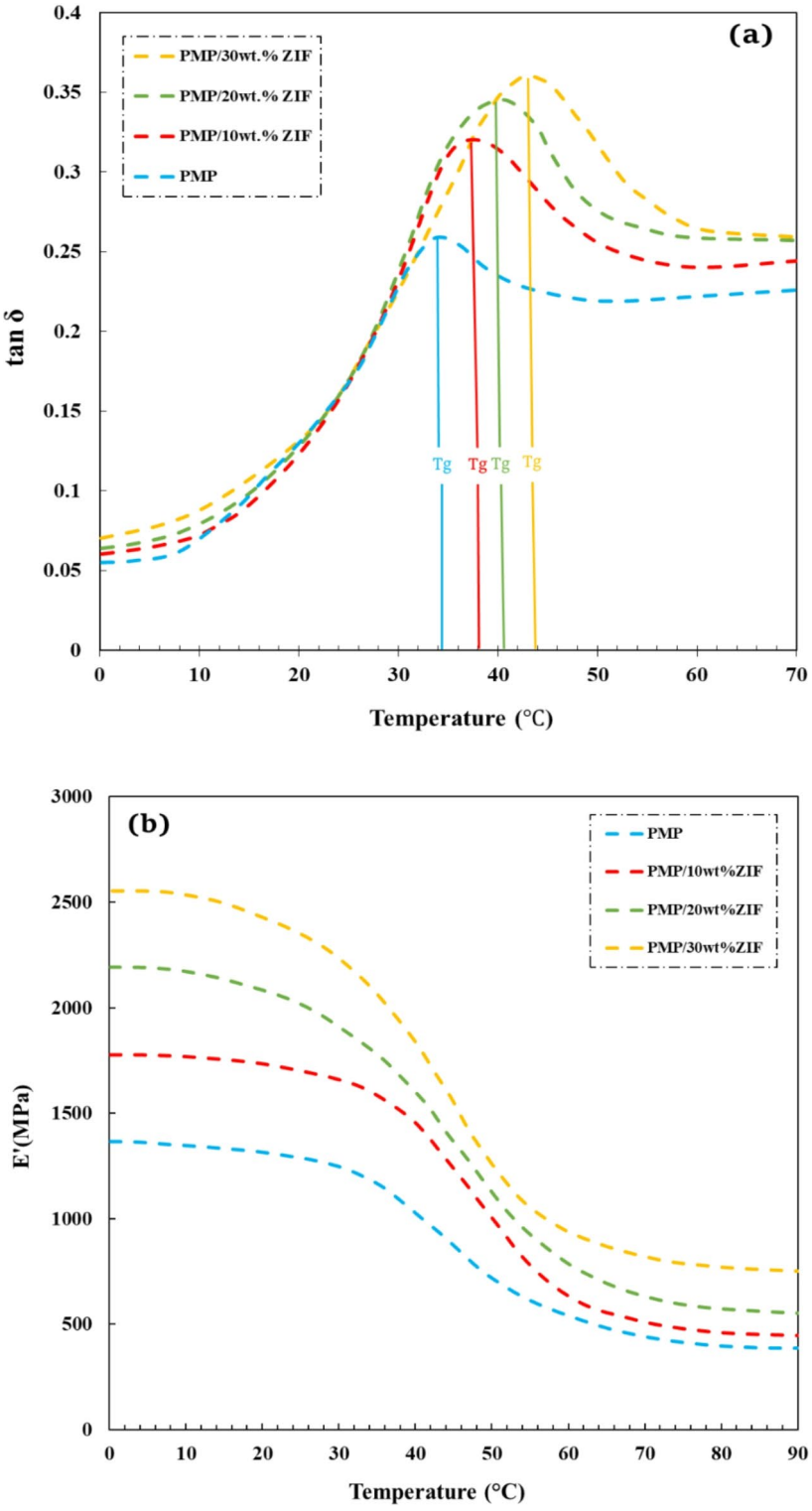

Fig. 5. (a) tan δ curve, (b) storage modulus versus temperature for PMP, PMP/10 wt% MOF, PMP/20 wt% MOF and PMP/30 wt% MOF.

between nanoparticles with CH_4 and H_2 gases, along with the very low condensability of these two gases, has led to an insignificant increase in their solubility[36,37].

The values of diffusion selectivity (D_{CO2}/D_{CH4}), (D_{CO2}/D_{H2}) and dissolution selectivity (S_{CO2}/S_{CH4}), (S_{CO2}/S_{H2}) are shown in Table 5. The dissolution selectivity increased with the addition of ZIF-8 nanoparticles, which has the main effect on the overall selectivity. The MOF in the polymer matrix separates the desired gases based on selective absorption, not based on screening properties, therefore, the dissolution selectivity value of $S_{CO2}/$

Membrane	Tensile strength (MPa)	Elongation at break (%)	Young modulus (GPa)
PMP	137 ± 2	121 ± 5	4.19 ± 0.2
PMP/10 wt% ZIF	126 ± 3	116 ± 2	4.72 ± 0.2
PMP/20 wt% ZIF	119 ± 2	108 ± 3	5.06 ± 0.1
PMP/30 wt% ZIF	107 ± 4	99 ± 3	5.44 ± 0.3

Table 3. Mechanical properties of ZIF-8 filled PMP membranes at different loadings.

Membrane Code	P (CO_2)	P (CH_4)	P (H_2)	CO_2/CH_4	CO_2/H_2
M1	99.13	7.38	8.52	13.43	11.63
M2	139.24	7.61	8.84	18.29	15.75
M3	194.32	7.95	9.01	24.44	21.56
M4	259.81	8.54	9.24	30.42	28.11

Table 4. Effect of ZIF-8 content on PMP/ZIF-8 membranes at 2 bar.

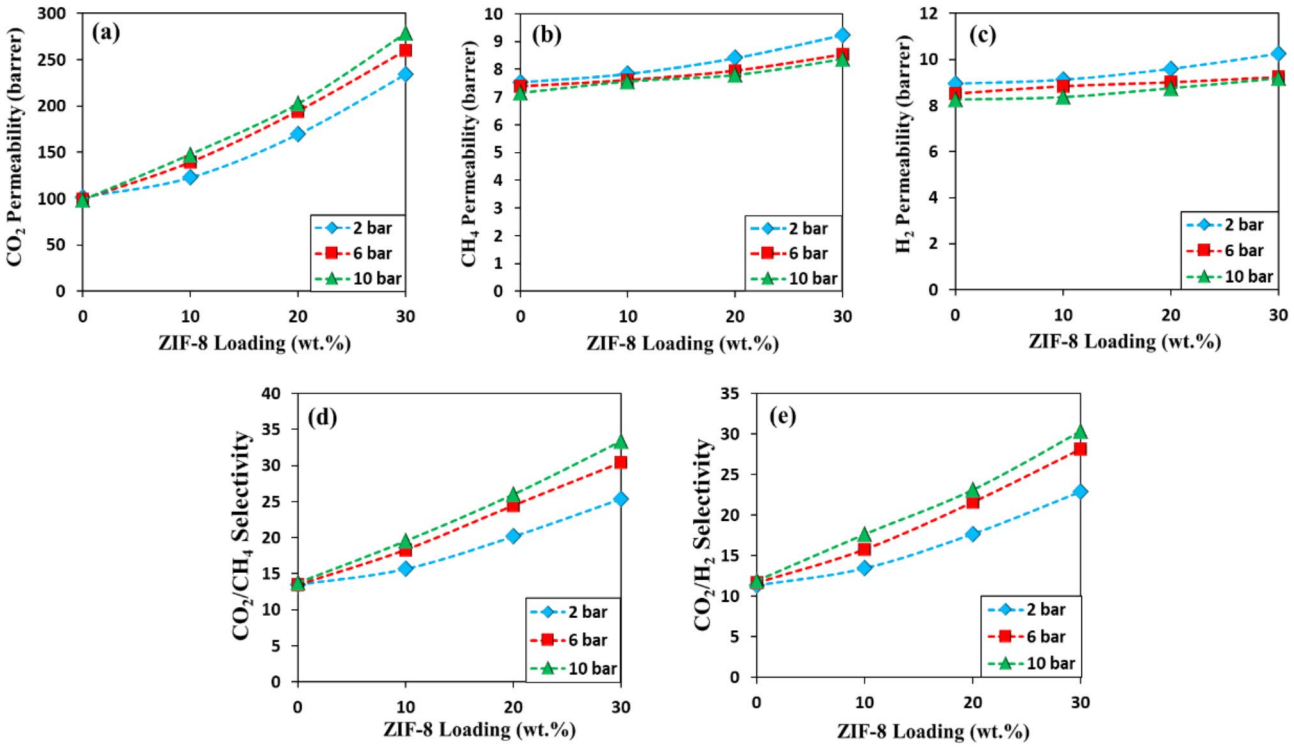

Fig. 6. The effect of ZIF-8 content and pressure changes on (**a**) CO_2 permeability, (**b**) CH_4 permeability, (**c**) H_2 permeability, (**d**) CO_2/CH_4 selectivity, and (**e**) CO_2/H_2 selectivity.

S_{CH4}=11.09 and S_{CO2}/S_{H2}=15.60 in PMP membrane increased to 20.05 and 26.29 in PMP/ZIF-8 membranes, respectively. The permeation of CH_4 and H_2 gases is reduced due to the hardening of PMP polymer chains and the lengthening of the permeation path (due to the presence of ZIF-8 nanoparticles), and as a result, permeation selectivity is improved from D_{CO2}/D_{CH4}=1.21 and D_{CO2}/D_{H2}=0.72 in PMP polymer membrane to 1.26 and 0.87 in PMP/ZIF-8 membranes, respectively. On the other hand, one of the characteristics of reverse selectivity membranes is the separation of gases based on solubility, and the contribution of permeation selectivity in gas separation is decreased. In the studied MMMs, the permeation selectivity values are close to one and its contribution to CO_2/CH_4 and CO_2/H_2 selectivity dwindled. According to the obtained results and the abovementioned explanations, it can be concluded that the PMP/ZIF-8 membrane possess better reverse selectivity properties.

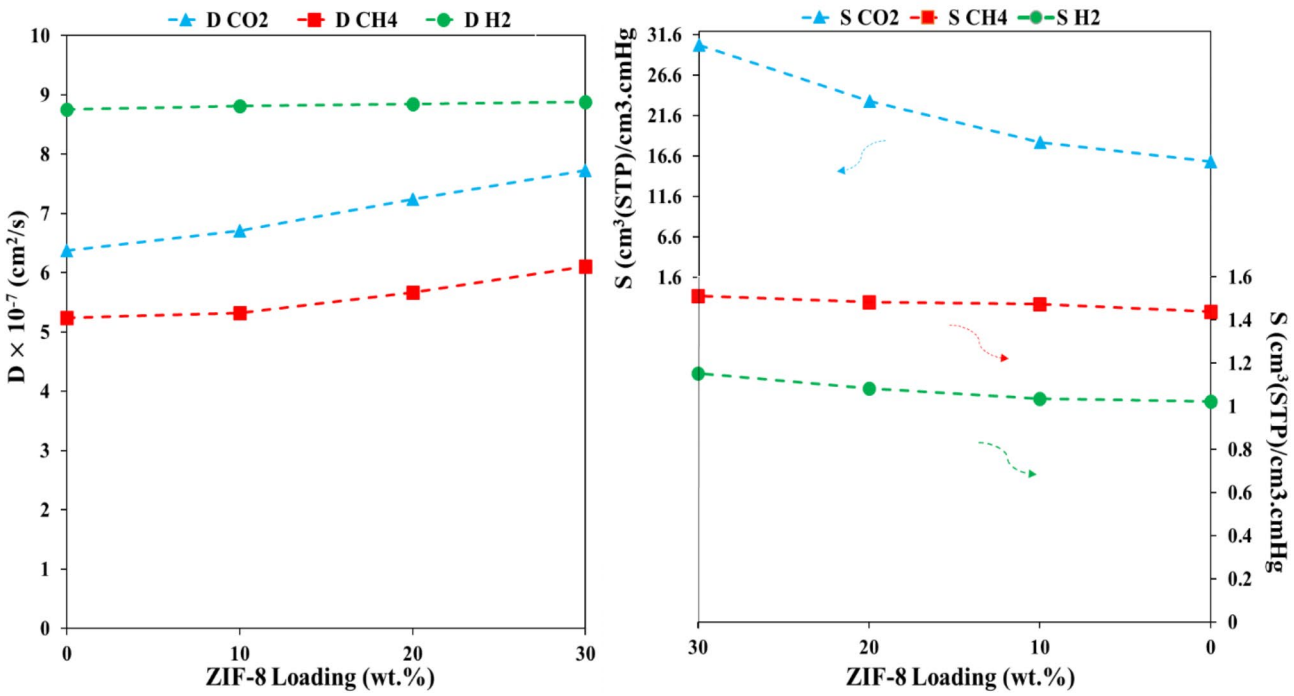

Fig. 7. the effect of filler loading on CO_2, CH_4 and H_2. Diffusion and solubility coefficients.

Membrane Code	D_{CO2}/D_{CH4}	D_{CO2}/D_{H2}	S_{CO2}/S_{CH4}	S_{CO2}/S_{H2}
M1	1.21	0.72	11.09	15.60
M2	1.26	0.76	12.42	17.68
M3	1.27	0.81	15.78	21.61
M4	1.26	0.87	20.05	26.29

Table 5. Effect of ZIF-8 content on PMP/ZIF-8 membranes at 2 bar.

Effect of pressure on the performance of MMMs in separation of CO_2/CH_4 and CO_2/H_2

Figure 8 indicates the effect of feed pressure on the permeability of CO_2, CH_4 and H_2 gases, as well as the selectivity of CO_2/CH_4 and CO_2/H_2 in polymer and mixed matrix membranes with varied weight percentages and at a temperature of 30 ℃. In the PMP polymer membrane, with the increase in pressure, the permeability of gases encountered a slight decrease; the permeability of CO_2 changed from 101.67 Barrer at a pressure of 2 bar to 99.13 Barrer at a pressure of 6 bar. The permeability of CH_4 and H_2 at a pressure of 2 bar decreased from 7.24 to 8.95 Barrer to 7.38 and 8.52 Barrer at 6 bar pressure, respectively. Increasing the pressure on the feed side densifies the polymer chains and as a result reduces the penetration of gases in the polymer network of the membrane, which can also result in a reduction in permeability. According to the figure, the permeability of CO_2 in the MMMs enhanced with the increase in the weight% of nanoparticles at higher pressures. For instance, the permeability of CO_2 in the membrane containing 30 wt% of ZIF-8 particles increased from 234.41 Barrer at 2 bar pressure to 259.81 Barrer at 6 bar pressure. This increasing trend in MMMs is only evident in CO_2 gas and is not seen in other gases. One of the main reasons for this variation in permeability is the increase in the concentration of condensable gases such as CO_2, which causes the softening phenomenon in the membrane. Figure 8 indicates the changes in selectivity of CO_2/CH_4 and CO_2/H_2 in pure PMP membrane and MMMs with different weight percentages, with respect to feed pressure. The increase in feed pressure improved the selectivity of CO_2/CH_4 and CO_2/H_2 in MMMs. The adsorption through MOF particles along with the condensation are considered the main factors of gas permeability variation in MMMs at higher pressures. Factors affecting the improvement of the selectivity of CO_2/CH_4 and CO_2/H_2 in membranes containing ZIF-8 particles, it can be mentioned the reduction of permeability of CH_4 and H_2 due to the hardening of polymer chains, especially in the polymer/particle joint phase[38].

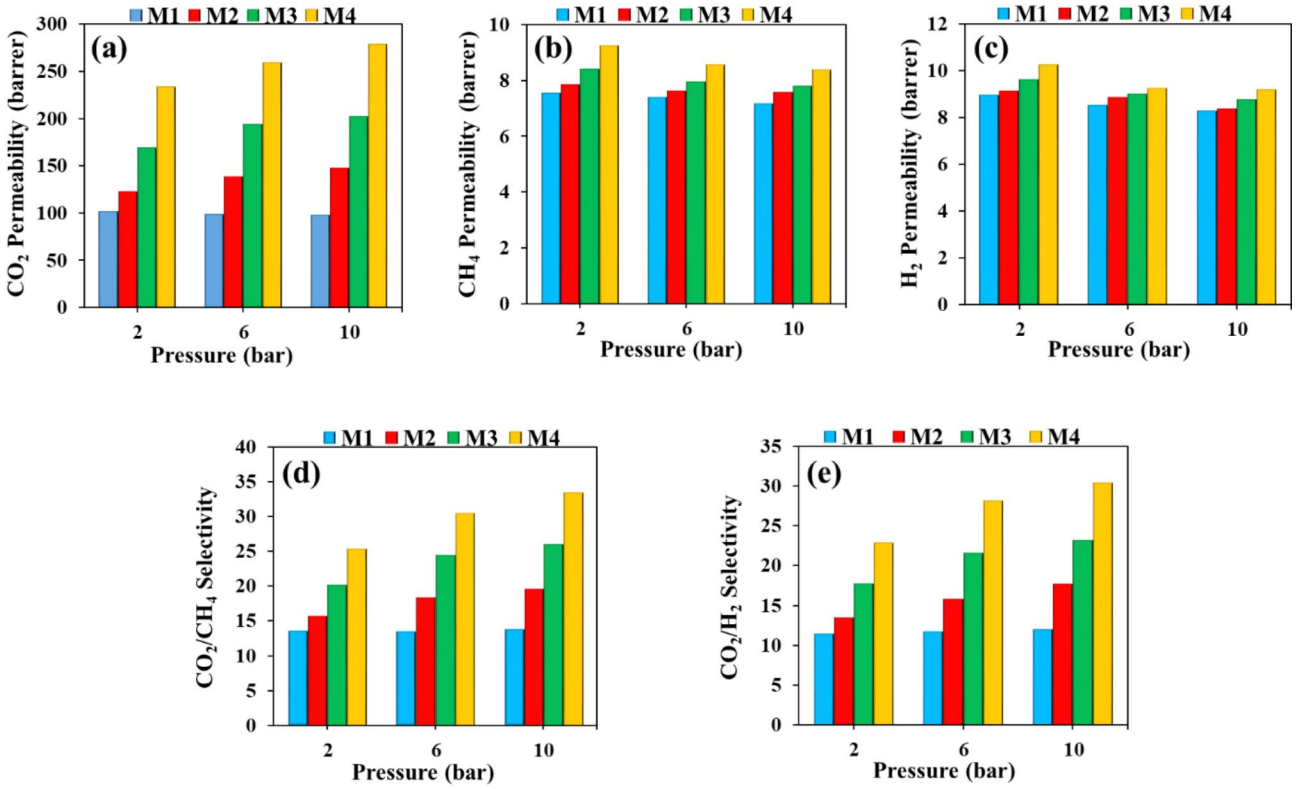

Fig. 8. The effect of pressure on permeability of (**a**) CO_2, (**b**) CH_4, (**c**) H_2 and selectivity of (**d**) CO_2/CH_4, (**e**) CO_2/H_2.

According to Fig. 9, the permeability coefficient for pure membranes and mixed matrix membranes slightly decreased with increasing pressure. At higher pressures, the membrane becomes denser and the free volume of the membrane decreases, which can lead to a reduction in the gas permeability coefficient[39]. For this reason, the diffusion coefficient of these gases did not have a noticeable dependence on the pressure change. Another factor which is affected by pressure variation is the solubility coefficient of gases. In general, increasing the gas pressure will increase the gas concentration upstream of the membrane and can have a more favorable effect on the gas solubility coefficient. CO_2 gas has higher compressibility compared to CH_4 and H_2 gases, this positive feature along with the favorable interactions of CO_2 with the prepared membranes significantly enhanced the solubility coefficient of this gas with increasing pressure. On the other hand, the pressure increase had no significant effect on the solubility coefficient of CH_4 and H_2 gases due to low compressibility and lack of proper interaction with the constructed membranes[40]. Figures 10 and 11 show the performance of pure membranes and mixed matrix membranes in the separation of CO_2/CH_4 and CO_2/H_2 compared to Robson's limit. According to the figure, better performance of the membrane is observed in the weight% and also at higher pressures, compared to Robson's limit.

Mixed gas tests

The mixed gas permeation properties of the PMP/ZIF-8 mixed matrix membranes (MMMs) were investigated using equimolar (50:50 v/v) gas mixtures of CO_2/CH_4 and CO_2/H_2. The experiments were conducted at a pressure of 6 bar and a temperature of 30 °C. After passing the gas mixture through the membrane, the impermeable flow was removed, and the composition of the permeable gas flow was determined using gas chromatography (GC). The permeability and selectivity results for the mixed gas conditions are presented in Table 6.

A comparison of the mixed gas permeability results with the pure gas data indicates a decline in CO_2 permeability and selectivity in all MMMs. This reduction is attributed to the competitive sorption and transport effects that arise in the presence of CH_4 and H_2 in the mixture.

This reduction occurs due to the presence of CH_4 and H_2 in the mixture, which inhibits CO_2 transport through the membrane. The decrease in permeability is more pronounced in MMMs with higher ZIF-8 loading, suggesting that ZIF-8 particles have a role in CO_2 adsorption competition. The ideal CO_2/CH_4 selectivity values for PMP/10, 20, and 30 wt% ZIF-8 were 18.29, 24.44, and 30.42, respectively. Under mixed gas conditions, these values reduced to 16.97, 23.63, and 29.71, respectively. Similarly, the ideal CO_2/H_2 selectivity decreased from 15.75, 21.56, and 28.11 in pure gas conditions to 14.76, 20.95, and 27.26, respectively, in mixed gas. The decrease in gas permeability and CO_2 selectivity over CH_4 and H_2 can be attributed to the following series of phenomena:

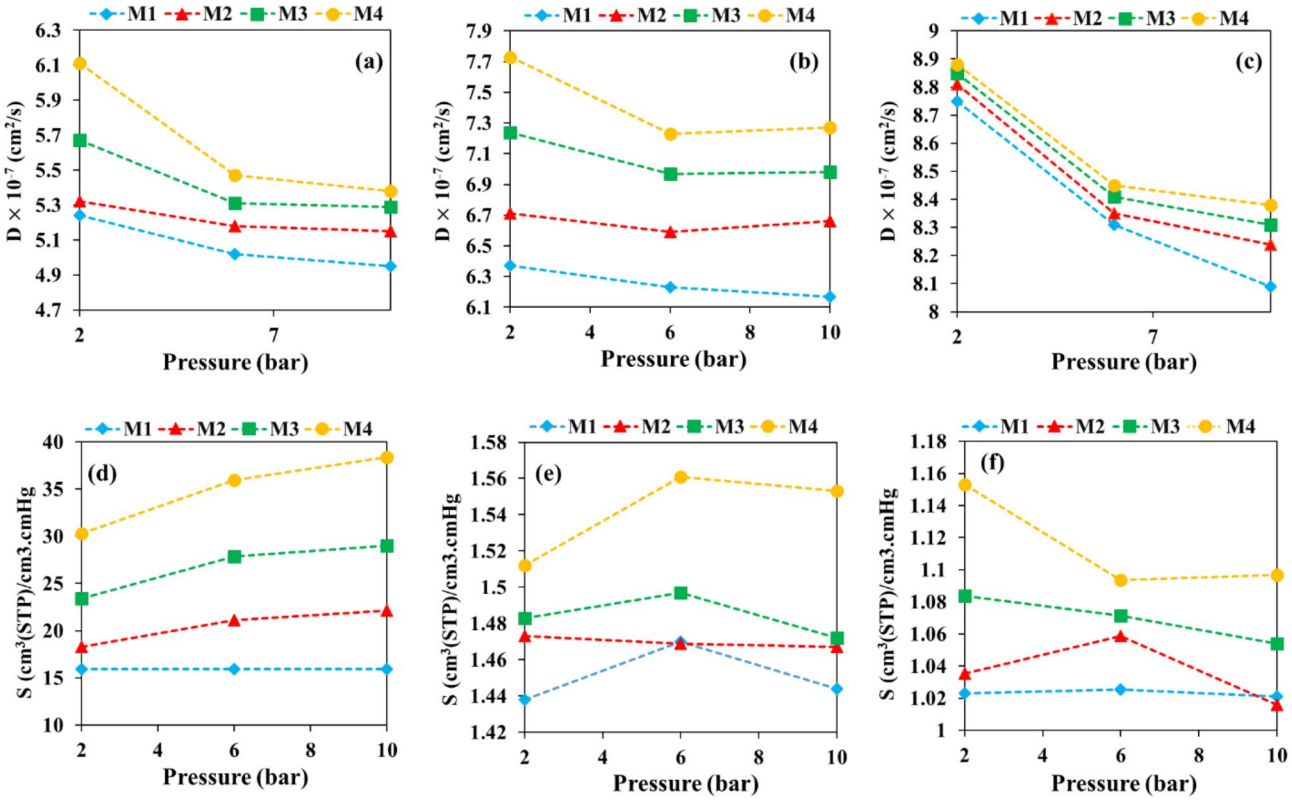

Fig. 9. The effect of pressure on diffusion coefficient of (**a**) CO_2, (**b**) CH_4, (**c**) H_2 and solubility coefficient of (**d**) CO_2, (**e**) CH_4, (**f**) H_2.

The presence of CH_4 in the gas mixture reduces CO_2 adsorption on the ZIF-8 particles. Since ZIF-8 has an affinity for CO_2, the simultaneous presence of CH_4 reduces the effective number of adsorption sites available for CO_2.

1. The presence of CH_4 in the gas mixture reduces CO_2 adsorption on the ZIF-8 particles. Since ZIF-8 has an affinity for CO_2, the simultaneous presence of CH_4 reduces the effective number of adsorption sites available for CO_2.
2. The presence of CH_4 inside the membrane matrix, especially within the free volume, inhibits the condensation of CO_2. This reduces the solubility of CO_2, thereby lowering its overall permeability.
3. In mixed gas conditions, CH_4 and H_2 molecules occupy free volume spaces within PMP, disrupting the CO_2 transport pathways.

Gas separation performance

The gas separation results of the prepared membranes were compared with the results of various articles about MMMs with Robseon's upper limit and the results are shown in Figs. 12 and 13. It was revealed that not only the gas separation properties of the fabricated MMMs in this research was better than most of the other reported MMMs, but also exceeded the upper limit of Robson, which confirms the optimal performance of the prepared membranes. In addition, outstanding results were obtained, even at low amount of nanoparticles, which can reduce the cost of membrane construction.

Conclusions

In this research, new MMMs were fabricated using ZIF-8 nanoparticles and PMP polymer. In order to evaluate the gas separation performance of the prepared membranes, a gas permeability test was conducted at a constant temperature of 30 ℃ and pressures of 2, 6 and 10 bar, using a constant volume-variable pressure device. In addition, various tests such as FESEM, FTIR-ATR, BET, TGA and DMTA were applied to investigate and analyze the structure of the membranes. The obtained results demonstrated that the nanoparticles had very good compatibility with the PMP polymer, with uniform distribution over the polymer bed without any accumulation. The polymer chains surrounded the nanoparticles without any holes or defects. Based on gas permeability results, the most appropriate performance was observed with MMMs containing 30% by weight of nanoparticles, in which CO_2 gas permeability improved by more than 180% compared to the pure polymer membrane at a pressure of 10 bar and reached about 278.95 Barrer. Meanwhile, the selectivity of CO_2/CH_4 and CO_2/H_2 improved by 142% and 155% respectively at 10 bar pressure and reached 33.36 and 30.35.

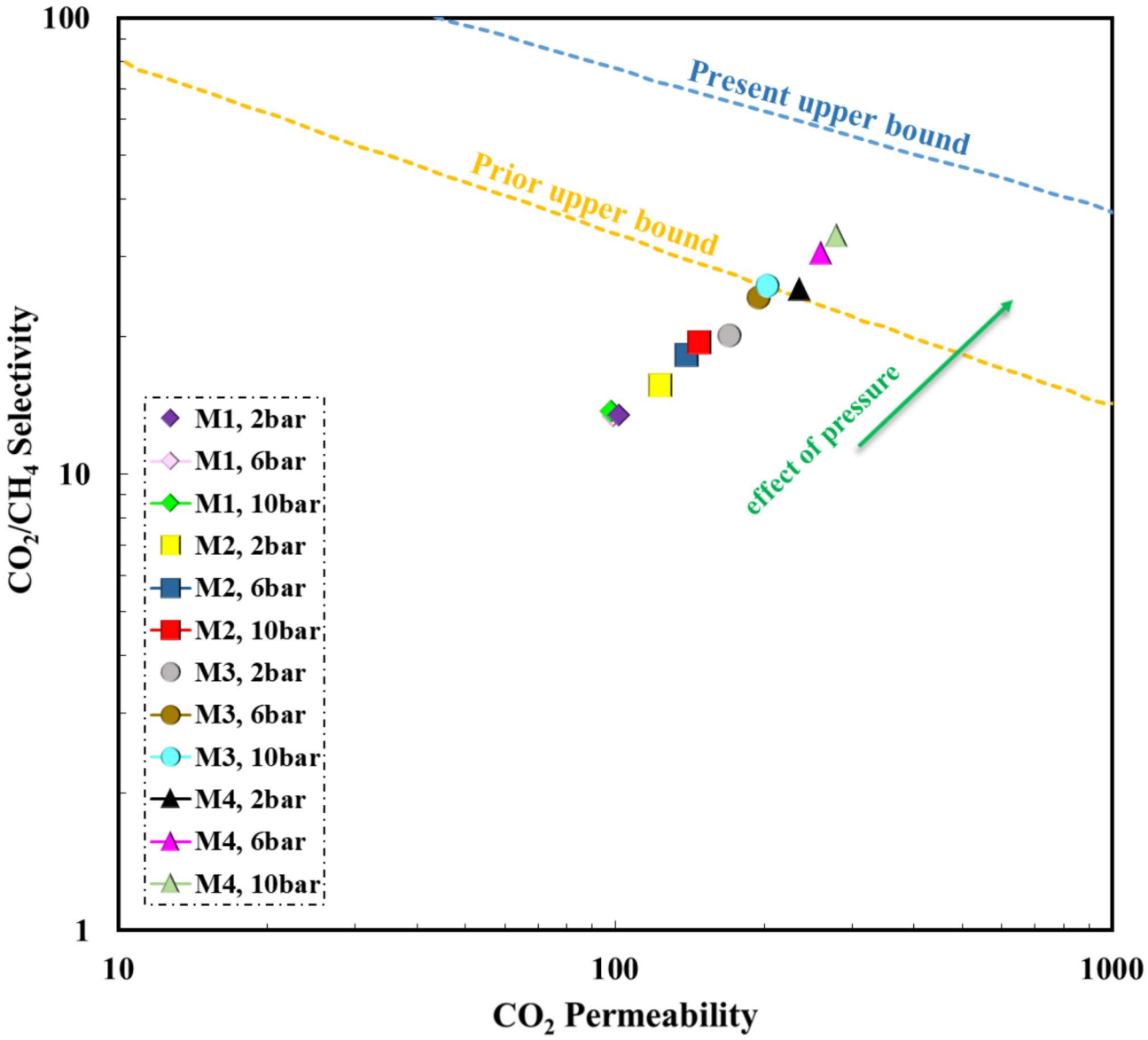

Fig. 10. Comparison of CO_2/CH_4 separation performances of pure PMP, PMP/ZIF-8 with Robeson present and prior bound.

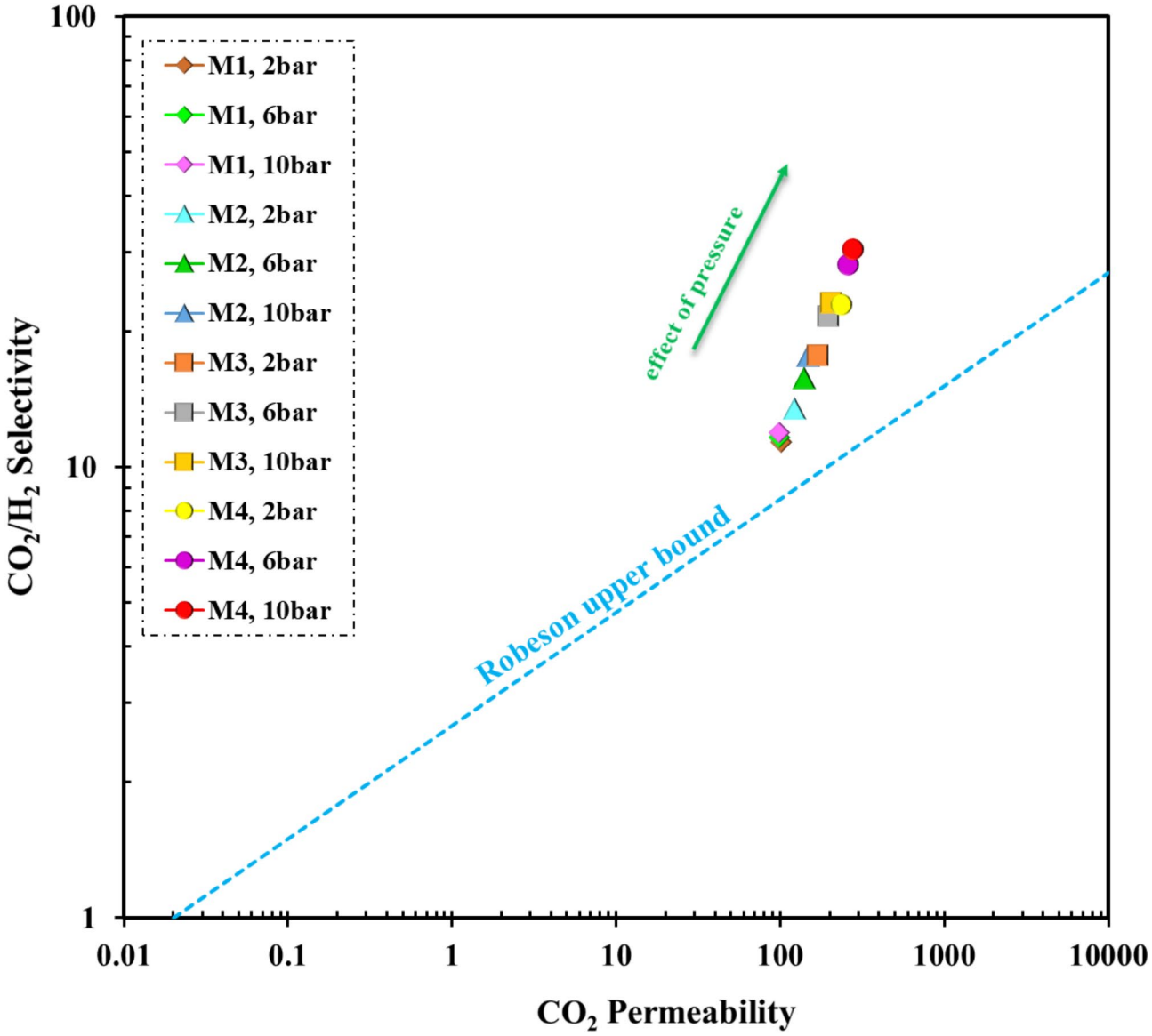

Fig. 11. Comparison of CO_2/H_2 separation performances of pure PMP, PMP/ZIF-8 with Robeson present and prior bound.

Pure gas tests					Mixed gas tests				
Permeability (barrer)			Ideal selectivity		Permeability (barrer)			Real selectivity	
CO_2	CH_4	H_2	CO_2/CH_4	CO_2/H_2	CO_2	CH_4	H_2	CO_2/CH_4	CO_2/H_2
PMP/10 wt% ZIF-8									
139.24	7.61	8.84	18.29	15.75	128.35	7.56	8.69	16.97	14.76
PMP/20 wt% ZIF-8									
194.32	7.95	9.01	24.44	21.56	185.26	7.84	8.84	23.63	20.95
PMP/30 wt% ZIF-8									
259.81	8.54	9.24	30.42	28.11	248.38	8.36	9.11	29.71	27.26

Table 6. Mixed gas permeability and selectivity data at 6 bar and 30 °C compared to pure gas tests.

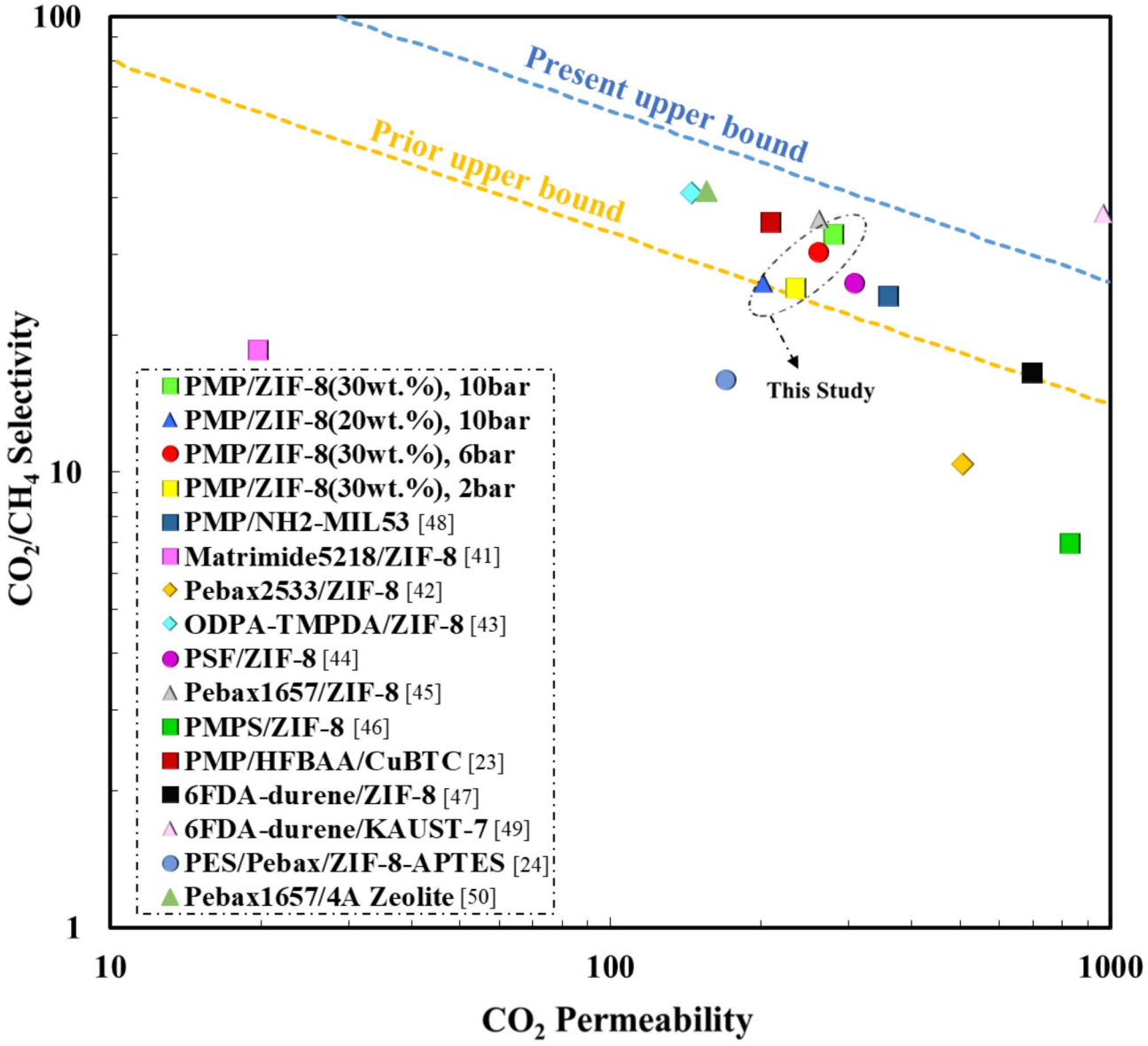

Fig. 12. A comparison between the results of the present study and other MMMs in CO_2/CH_4 separation.

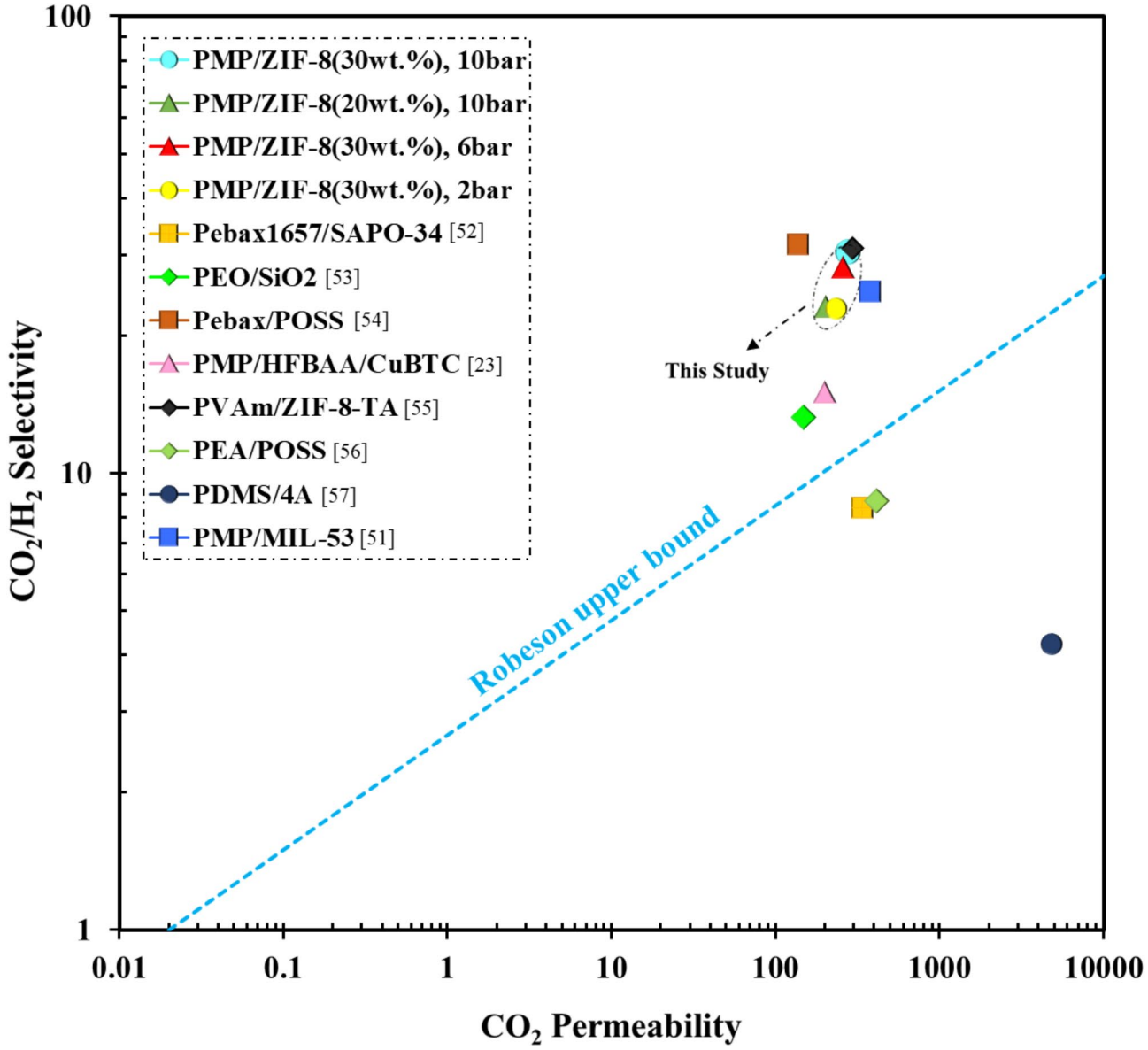

Fig. 13. A comparison between the results of the present work and other MMMs in CO_2/H_2 separation.

Data availability

All data generated or analysed during this study are included in this published article.

Received: 25 December 2024; Accepted: 19 March 2025
Published online: 25 April 2025

References

1. Nematollahi, M. H. et al. Recent progress on pebax-based thin film nanocomposite membranes for CO_2 capture: the state of the art and future outlooks. *Energy Fuels.* **36**(20), 12367–12428 (2022).
2. Ranjbar, F. et al. The experimental/theoretical study over the effect of using the POP-NH. *Nanostruct. Into Membrane Selective Layer. CO2 Permeability Selectivity Chem. Eng. Res. Des.* **187**, 184–195 (2022).
3. Zhu, T. et al. Preparation of poly (ether-block-amide)/poly (amide-co-poly (propylene glycol)) random copolymer blend membranes for CO_2/N_2 separation. *Polym. Eng. Sci.* **59**, 14–23 (2019).
4. Tajdini, Z. & Feijani, E. A. Highly promoted CO_2 separation of poly (ether-block-amide) based mixed matrix membranes using MOFs@ aminoclay architectures as fillers. *Sci. Rep.* **14**(1), 29082 (2024).
5. Hassanzadeh, H., Abedini, R. & Ghorbani, M. CO_2 separation over N_2 and CH_4 light gases in sorbitol-modified Poly (ether-block-amide)(pebax 2533) membrane. *Ind. Eng. Chem. Res.* **61**(36), 13669–13682 (2022).
6. Jumaah, A. F. & Abedini, R. Fabrication and performance evaluation of mixed matrix membrane comprising Pebax and graphene hydroxyl in olefin/paraffin separation. *Polyolefins J.* **12**, 31–44 (2025).
7. Zhu, T. et al. Random and block copolymer membranes based on flexible etheric-aliphatic soft segments designed for CO_2/CH_4 separation. *J. Nat. Gas Sci. Eng.* **54**, 92–101 (2018).

8. Doosti, M. & Abedini, R. Polyethyleneglycol-modified cellulose acetate membrane for efficient olefin/paraffin separation. *Energy Fuels*. **36**(17), 10082–10095 (2022).
9. Noorani, N., Mehrdad, A. & Shamszadeh, P. PVC-based mixed-matrix membranes based on IL@ AC/ NH_2-MIL-101 nanocomposites for improved CO_2 separation performance. *Sci. Rep.* **14**(1), 23843 (2024).
10. Kheirtalab, M., Abedini, R. & Ghorbani, M. Pebax/poly (vinyl alcohol) mixed matrix membrane incorporated by amine-functionalized graphene oxide for CO_2 separation. *J. Polym. Sci.* **62**(3), 517–535 (2024).
11. Zhang, D. S. et al. Fluorous metal-organic frameworks with enhanced stability and high H_2/CO_2 storage capacities. *Sci. Rep.* **3**(1), 3312 (2013).
12. Behera, A. Metal-organic frameworks. In *Advanced Materials. P* 637–666 (Springer, 2022).
13. Khoshhal Salestan, S., Rahimpour, A. & Abedini, R. Experimental and theoretical studies of biopolymers on the efficient CO_2/CH_4 separation of thin-film Pebax® 1657 membrane. *Chem. Eng. Processing-Process Intensif.* **163**, 108366 (2021).
14. Abdollahi, S. A. & Ranjbar, S. F. Modeling the CO_2 separation capability of Poly (4-methyl-1-pentane) membrane modified with different nanoparticles by artificial neural networks. *Sci. Rep.* **13**(1), 8812 (2023).
15. Xiao, Y. et al. The strategies of molecular architecture and modification of polyimide-based membranes for CO_2 removal from natural gas—A review. *Prog. Polym. Sci.* **34**(6), 561–580 (2009).
16. Merkel, T. et al. Ultrapermeable, reverse-selective nanocomposite membranes. *Science*. **296**(5567), 519–522 (2002).
17. Golubev, G. S. et al. High free volume polymers for pervaporation. *Curr. Opin. Chem. Eng.* **36**, 100788 (2022).
18. Lau, C. H. et al. Reverse-selective polymeric membranes for gas separations. *Prog. Polym. Sci.* **38**(5), 740–766 (2013).
19. Cohen, M. H. & Turnbull, D. Molecular transport in liquids and glasses. *J. Chem. Phys.* **31**(5), 1164–1169 (1959).
20. Sun, L. et al. N self-doped ZnO derived from microwave hydrothermal synthesized zeolitic imidazolate framework-8 toward enhanced photocatalytic degradation of methylene blue. *J. Colloid Interface Sci.* **565**, 142–155 (2020).
21. Abedini, R., Mosayebi, A. & Mokhtari, M. Improved CO_2 separation of Azide cross-linked PMP mixed matrix membrane embedded by nano-CuBTC metal organic framework. *Process Saf. Environ. Prot.* **114**, 229–239 (2018).
22. Amedi, H. R. & Aghajani, M. Functionalized Zeolitic-Imidazole Frameworks-8 based Poly (ether-b-amide) nanocomposite membrane for CO_2/CH_4 gas separation: synthesis and characterization. *Iran. J. Polym. Sci. Technol.* **31**, 3–14 (2018).
23. Zhu, T. et al. ZIF-8@ GO composites incorporated polydimethylsiloxane membrane with prominent separation performance for ethanol recovery. *J. Membr. Sci.* **598**, 117681 (2020).
24. Nematollahi, M. H., Babaei, S. & Abedini, R. CO_2 separation over light gases for nano-composite membrane comprising modified polyurethane with SiO_2 nanoparticles. *Korean J. Chem. Eng.* **36**, 763–779 (2019).
25. Shirzad Kebria, M. R. et al. Experimental and theoretical investigation of thin ZIF-8/chitosan coated layer on air gap membrane distillation performance of PVDF membrane. *Desalination*. **450**(15), 21–32. (2019).
26. Nobakht, D. & Abedini, R. A new ternary Pebax® 1657/maltitol/ZIF-8 mixed matrix membrane for efficient CO_2 separation. *Process Saf. Environ. Prot.* **170**, 709-719 (2023).
27. Mansourpanah, Y. & Bagri, F. Improvement of the performance of PDMS top layer of mixed matrix membrane incorporated with treated ZIF-8 for gas separation. *J. Membrane Sci. Res.* **7**(2), 111–117 (2021).
28. Fakoori, M. et al. Effect of Cu-MOFs incorporation on gas separation of Pebax thin film nanocomposite (TFN) membrane. *Korean J. Chem. Eng.* **38**, 121–128 (2021).
29. Zhang, H., Zhao, M. & Lin, Y. Stability of ZIF-8 in water under ambient conditions. *Microporous Mesoporous Mater.* **279**, 201–210 (2019).
30. Lee, Y. R. et al. ZIF-8: A comparison of synthesis methods. *Chem. Eng. J.* **271**, 276–280 (2015).
31. Hu, Y. et al. Amino-functionalized multiple-walled carbon nanotubes-polyimide nanocomposite films fabricated by in situ polymerization. *J. Appl. Polym. Sci.* **110**(2), 701–705 (2008).
32. Babaei, S., Nematollahi, M. H. & Abedini, R. Pure and mixed gas permeation study of silica incorporated polyurethane-urea membrane modified by Moca chain extender. *Can. J. Chem. Eng.* **98**, 1543–1557 (2020).
33. Zhu et al. Facile covalent crosslinking of zeolitic imidazolate framework/polydimethylsiloxane mixed matrix membrane for enhanced ethanol/water separation performance. *ACS Sustain. Chem. Eng.* **8**, 12664–12676 (2020).
34. Dai, Z. et al. Poly (1-trimethylsilyl-1-propyne)-based hybrid membranes: effects of various nanofillers and feed gas humidity on CO_2 permeation. *Membranes* **8**(3), 76 (2018).
35. Mozafari, M., Rahimpour, A. & Abedini, R. Exploiting the effects of zirconium-based metal organic framework decorated carbon nanofibers to improve CO2/CH4 separation performance of thin film nanocomposite membranes. *J. Ind. Eng. Chem.* **85**, 102–110 (2020).
36. Nematollahi, M. H., Dehaghani, A. H. S. & Abedini, R. CO_2/CH_4 separation with Poly (4-methyl-1-pentyne)(TPX) based mixed matrix membrane filled with Al_2O_3 nanoparticles. *Korean J. Chem. Eng.* **33**(2), 657–665 (2016).
37. Kalantari, S. et al. Superior interfacial design in ternary mixed matrix membranes to enhance the CO_2 separation performance. *Appl. Mater. Today*. **18**, 100491 (2020).
38. Pakizeh, M. et al. Preparation and characterization of dimethyldichlorosilane modified Si O_2/PSf nanocomposite membrane. *Korean J. Chem. Eng.* **30**(3), 751–760 (2013).
39. Ghasemi Estahbanati, E., Omidkhah, M. & Ebadi Amooghin, A. Interfacial design of ternary mixed matrix membranes containing Pebax 1657/silver-nanopowder/[BMIM][BF4] for improved CO_2 separation performance. *ACS Appl. Mater. Interfaces.* **9**(11), 10094–10105 (2017).
40. Kheirtalab, M., Abedini, R. & Ghorbani, M. A novel ternary mixed matrix membrane comprising polyvinyl alcohol (PVA)-modified poly (ether-block-amide)(Pebax® 1657)/graphene oxide nanoparticles for CO_2 separation. *Process Saf. Environ. Prot.* **144**, 208–224 (2020).
41. Song, Q. et al. Zeolitic imidazolate framework (ZIF-8) based polymer nanocomposite membranes for gas separation. *Energy Environ. Sci.* **5**(8), 8359–8369 (2012).
42. Nafisi, V. & Hägg, M. B. Development of dual layer of ZIF-8/PEBAX-2533 mixed matrix membrane for CO_2 capture. *J. Membr. Sci.* **459**, 244–255 (2014).
43. Li, W., Samarasinghe, S. A. S. C. & Bae, T. H. Enhancing CO_2/CH_4 separation performance and mechanical strength of mixed-matrix membrane via combined use of graphene oxide and ZIF-8. *J. Ind. Eng. Chem.* **67**, 156–163 (2018).
44. Ban, Y. et al. Confinement of ionic liquids in nanocages: tailoring the molecular sieving properties of ZIF-8 for membrane-based CO_2 capture. *Angew. Chem. Int. Ed.* **54**(51), 15483–15487 (2015).
45. Jomekian, A. et al. Ionic liquid-modified Pebax® 1657 membrane filled by ZIF-8 particles for separation of CO_2 from CH_4, N_2 and H_2. *J. Membr. Sci.* **524**, 652–662 (2017).
46. Diestel, L. et al. Comparative permeation studies on three supported membranes: pure ZIF-8, pure polymethylphenylsiloxane, and mixed matrix membranes. *Microporous Mesoporous Mater.* **189**, 210–215 (2014).
47. Jusoh, N. et al. Transport properties of mixed matrix membranes encompassing zeolitic imidazolate framework 8 (ZIF-8) nanofiller and 6FDA-durene polymer: optimization of process variables for the separation of CO_2 from CH_4. *J. Clean. Prod.* **149**, 80–95 (2017).
48. Abedini, R., Omidkhah, M. & Dorosti, F. Highly permeable Poly (4-methyl-1-pentyne)/ NH_2-MIL 53 (Al) mixed matrix membrane for CO_2/CH_4 separation. *RSC Adv.* **4**, 36522–36537 (2014).
49. Chen, K. et al. Enhanced CO_2/CH_4 separation performance of mixed-matrix membranes through dispersion of sorption-selective MOF nanocrystals. *J. Membr. Sci.* **563**, 360–370 (2018).

50. Murali, R. S. et al. Mixed matrix membranes of Pebax-1657 loaded with 4A zeolite for gaseous separations. *Sep. Purif. Technol.* **129**, 1–8 (2014).
51. Abedini, R., Omidkhah, M. & Dorosti, F. Hydrogen separation and purification with poly (4-methyl-1-pentyne)/MIL-53 mixed matrix membrane based on reverse selectivity. *Int. J. Hydrog. Energy*. **39**(15), 7897–7909 (2014).
52. Zhao, D. et al. Poly (amide-6-b-ethylene oxide)/SAPO-34 mixed matrix membrane for CO_2 separation. *J. Energy Chem.* **23**(2), 227–234 (2014).
53. Shao, L. & Chung, T. S. In situ fabrication of cross-linked PEO/silica reverse-selective membranes for hydrogen purification. *Int. J. Hydrog. Energy*. **34**(15), 6492–6504 (2009).
54. Li, Y. & Chung, T. S. Molecular-level mixed matrix membranes comprising Pebax® and POSS for hydrogen purification via preferential CO_2 removal. *Int. J. Hydrog. Energy*. **35**(19), 10560–10568 (2010).
55. Chen, F. et al. Preparation of mixed matrix composite membrane for hydrogen purification by incorporating ZIF-8 nanoparticles modified with Tannic acid. *Int. J. Hydrog. Energy*. **45**(12), 7444–7454 (2020).
56. Chua, M. L. et al. Polyetheramine–polyhedral oligomeric Silsesquioxane organic–inorganic hybrid membranes for CO_2/H_2 and CO_2/N_2 separation. *J. Membr. Sci.* **385**, 40–48 (2011).
57. Rezakazemi, M., Shahidi, K. & Mohammadi, T. Hydrogen separation and purification using crosslinkable PDMS/zeolite A nanoparticles mixed matrix membranes. *Int. J. Hydrog. Energy*. **37**(19), 14576–14589 (2012).

Acknowledgements

The authors acknowledge Babol Noshirvani University of Technology for financial support of this project (Grant NO. BNUT/393054/2021).

Author contributions

Authors' contributionsThe authors' contributions are shown as below: Behnam Majid-Nateri: Methodology, Validation, Formal analysis, Investigation, Writing – original draft, Visualization. Reza Abedini: Conceptualization, Methodology, Validation, Formal analysis, Resources, Data curation, Writing – review & editing, Supervision, Project administration, Funding acquisition. Alireza Amiri: Validation, Formal analysis, Investigation, Writing – original draft, Visualization.

Declarations

Competing interests

The authors declare no competing interests.

Additional information

Correspondence and requests for materials should be addressed to R.A.

Reprints and permissions information is available at www.nature.com/reprints.

Publisher's note Springer Nature remains neutral with regard to jurisdictional claims in published maps and institutional affiliations.